BIBECHANA
Vol. 22, No. 3, December 2025, 215-222

ISSN 2091-0762 (Print), 2382-5340 (Online)
Journal homepage: http://nepjol.info/index.php/BIBECHANA
Publisher:Dept. of Phys., Mahendra Morang A. M. Campus (Tribhuvan University)Biratnagar

First-principles investigation of graphitic carbon nitride (GCN)monolayer embedded with transition metals (Ni, Pd, and Pt) as a NO sensor

Guna Nidhi Poudel, Pitamber Shrestha, Narayan Prasad Rijal, Shree Ram Sharma, Leela Pradhan Joshi, Rajendra Parajuli*

Department of Physics, Amrit Campus, Tribhuvan University, Kathmandu, Nepal
*Corresponding author. Email: rajendra.parajul@ac.tu.edu.np

Abstract

Adsorption of nitric oxide on Ni, Pt, and Pd-embedded graphitic carbon nitride (GCN) has been studied computationally using density functional theory. Transition metal (TM) embedded in GCN exhibits significantly higher adsorption energy compared to pristine GCN. This study finds that Pt-embedded GCN shows a high adsorption energy of -4.560 eV, which is greater than that of other TM-embedded GCNs. While NO gas showed physisorption on the pristine GCN, it exhibited strong chemisorption on the TM-embedded systems. When functional transitional metals are embedded on its surface, along with the adsorption of NO, new energy states are introduced near the Fermi surface, which modifies the electronic properties of the system. Also, the changes in the band states of the system are noticed. Furthermore, non-magnetic GCN is found to be magnetic when Pt is embedded in it.

Keywords
DFT, Graphitic Carbon Nitride (GCN), Electronic and Magnetic Properties, Adsorption.

Article information
Manuscript received: November 24, 2024; Revised July 29, 2025; Accepted: August 3, 2025
DOI https://doi.org/10.3126/bibechana.v22i3.71498

1 Introduction

The rapid growth of industrialization and vehicles around the globe has been one of the major sources of pollutant gasses such as CO, NO_2, SO_2, O_3, NO, etc., and NO [1] is considered one of the most threatening ones. This gas affects the environment heavily and negatively impacts the ecological balance and human health [2]. As the concentration of NO [3] in the atmosphere has increased rapidly over the past few years, it has been tantamount to developing a cheap, environment-friendly, and efficient technique to remove or at least effectively reduce such a pollutant gas from the atmosphere. Several attempts have been made to address this problem using catalytic processes and various other techniques [4]. However, the effectiveness of these approaches remains highly uncertain. Materials that possess properties such as chemical inertness, hardness, high surface area, and a tunable band gap have shown promise in adsorbing pollutants like nitric oxide (NO). Graphitic Carbon Nitride (GCN), a two-dimensional and layered material composed of carbon and nitrogen atoms, is found to have those

properties.

A Graphitic Carbon Nitride (GCN) sheet is composed of carbon and nitrogen atoms with sp^2 hybridization [5, 6] where the bond of partial N atoms is connected with two neighbors, and the C atom remains unsaturated [7, 8]. This enables it to adsorb foreign elements, molecules, etc. to gain stability. There are two types of structures of GCN, tri-s-triazine (C_6N_7) and triazine (C_3N_3), of which the former is the stable structure, and because of this, GCN nanosheets have been reported in the literature with remarkable interest concerning their adsorption behavior, catalysis, and photo catalysis [9, 10]. The space between the triazine group in GCN is the important center for the trapping of the cations, transitional metal, and the molecule with large radii inside it [11].

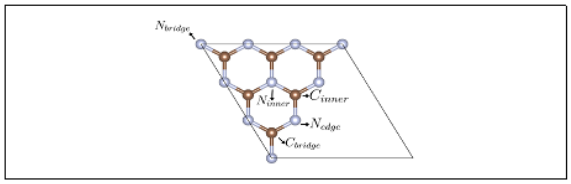

Figure 1: The optimized structure of unit cell of GCN.

D.K. Gorai et al. [2] studied the adsorption behavior of NO gas over Os, Ir, and Pt embedded-GCN by VASP software with PBE-GGA exchange correlation. They have found that NO is adsorbed physically with GCN but chemically with Os, Ir, and Pt-embedded GCN. They concluded that the Ir-embedded GCN can be considered a promising candidate for sensing NO gas and its elimination from the atmosphere. Basharnavaz et al. [3] studied Fe, Ru, and Os-embedded GCN for the NO gas sensor by using the Quantum Espresso simulation package. These authors found that Os -Os-embedded GCN is the promising candidate for the elimination of the NO gas from the environments as compared to the other two metals-embedded GCN. Xu et al. [12] studied the adsorption behavior and electronic states of poisonous gas molecules, like HCN, SO_2, H_2S, and NO, on GCN and Mo atom-embedded GCN. Further, the study of charge transfer analysis in their report indicates that H_2S acts as a donor, while HCN, SO_2, and NO act as acceptors. Density of States (DOS) study shows that HCN, SO_2, and H2S make the system inclined towards semimetallic, while the adsorption of NO onto Mo-embedded GCN contributes to smaller magnetic properties. Furthermore, Basharnavaz et al. [13] reported the adsorption properties of SO_2 gases over the transition metal/P–codoped GCN with Quantum Espresso software. Also, they reported that in transition metal (Co, Rh, and Ir), Ir/P–codoped system with the highest E_{ads} i.e. 3.52 eV can be effectively used for the removal and sensing of SO_2 gas from the polluted environment. Similarly, to explore high photocatalytic activity Gu et. al. [14] adopted the carbon vacancies and hydroxyls in GCN. The authors found from both computational and experimental characterization that the removal of photocatalytic NO from the CH-CN nanosheet was heavily attributed to the synergistic effects of carbon vacancies and hydroxyls. Metals such as Ag-, Li-, Na-, and K-doped GCN demonstrate the highest adsorption energy for NO_2 as investigated by Zhang and co-workers [15] by using the DMol3 package. They concluded their research by alluding that Ag-, Li-, Na-, and K-doped GCN are potential candidates for gas molecule sensors with unique and high sensitivity for NO_2. Furthermore, Basharnavaz et al. [16] investigated NO_2 adsorption behavior on Co, Rh, and Ir-embedded GCN, whereas transition metal-embedded GCN shows chemisorption of NO_2 gas with dramatic changes in conductivity and a large reduction in band gap energy. Their result shows that the wrinkle structure of TM-embedded GCN is found to exhibit a sharp close peak near the Fermi level and the huge amount of charge transferred from d-orbitals of the TM atoms to p orbitals of NO_2 gas.

Apart from the above-mentioned reports, GCN as an adsorbent with various adsorbates, including metal embedded GCN, has been documented in many literature. In one of the previous works [2], it has been extensively studied for Pt-embedded GCN; however, Ni and Pd-embedded GCN monolayers as NO gas sensors have not been reported so far. Our main objective in this paper is to compare Pt-embedded GCN as a NO sensor with the aforementioned relevant reports and to perform similar types of work with Pd and Ni-embedded GCN.

2 Computational Details

Ab initio calculations have been performed by Vienna Ab initio Simulation Package (VASP) [17] with Generalized Gradient Approximation (GGA) by using exchange-correlation functional Perdew-Burke Ernzerhor (PBE) [18]. The k-point sampling of the Brillouin zone was obtained using a 5×5×1 grid centered at the gamma (Γ) point using the Monkhorst Pack Scheme [19]. To depict the interactions between ion cores and valence electrons, we utilized the PAW potential as a pseudopotential [20, 21]. Kinetic energy cutoff 550eV is set up for plane-wave basis set expansion, limiting the total number of plane waves in calculations. We maintained system stability by implementing a convergence constraint of 10^7 eV in energy difference between successive self-consistent total energy calculation.

Table 1: Band gap (E_g) in eV, adsorption energy (E_{ads}) in eV, magnetic moment (M_{tot}) in μ_B, the distance between N and O ($d_{\text{N–O}}$) in Å, the distance between TM = Ni, Pd, Pt and N of NO ($d_{\text{TM–N}}$) in Å, the distance between TM = Ni, Pd, Pt and N_{edge} of GCN ($d_{\text{TM–Ned}}$) in Å.

Property	E_g (eV)	E_{ads} (eV)	M_{tot} (μ_B)	$d_{\text{N–O}}$ (Å)	$d_{\text{TM–N}}$ (Å)	$d_{\text{TM–Ned}}$ (Å)
NO	–	–	–	1.170	–	–
GCN	1.300	–	–	–	–	–
GCN-Ni	0.710	–	–	–	–	1.83
GCN-Pd	0.150	–	–	–	–	2.00
GCN-Pt	0.120	–	1.4000	–	–	1.92
GCN-Pt [2]	0.068	–	1.6641	–	–	2.384
GCN-NO	1.120	-0.807	–	1.171	–	–
GCN-Ni/NO	0.540	-4.270	0.0000	1.173	1.60	1.87
GCN-Pd/NO	0.100	-4.386	0.0000	1.175	1.72	2.03
GCN-Pt/NO	0.090	-4.560	0.0001	1.180	1.76	2.04
GCN-Pt/NO [2]	0.000	-4.790	0.0004	1.182	1.742	2.207

After applying these criteria, all atoms in the structures were allowed to relax, and subsequent calculations were carried out. However, the tetrahedron method was used to compute the band structure and density of state (DOS) calculations. For band structure computations, a set of 50 k-points was specifically chosen to span the high-symmetry points connecting the reciprocal space. This selection allows for a detailed analysis of how the energy bands evolve along this path in reciprocal space. To perform density of state calculations, the reciprocal space K point grid ($20 \times 20 \times 1$) was selected.

The adsorption energy E_{ads} for the adsorption of NO gas over the GCN system is calculated from:

$$E_{ads} = E_{GCN-NO} - (E_{GCN} + E_{NO}) \quad (1)$$

where $E_{GCN\text{-}NO}$ is the total energy of GCN with NO, E_{GCN} is the total energy of GCN and E_{NO} is the total energy of an isolated NO gas.

Similarly, E_{ads} for adsorption of NO gas over TM (Ni, Pd, Pt)-GCN system is calculated from:

$$E_{ads} = E_{TM-GCN-NO} - (E_{GCN} + E_{NO} + E_{TM}) \quad (2)$$

where $E_{TM\text{-}GCN\text{-}NO}$ is the total energy of TM-GCN with NO, E_{GCN} is the total energy of GCN, E_{NO} is the total energy of an isolated NO gas and E_{TM} is the energy of transition metal. A negative value is related to the exothermic process, and the adsorption process becomes thermodynamically stable.

3 Results and Discussion

The previous studies illustrated that the heptazine-based structure is more favorable than the triazine-based structure [22,23]. The optimized structure of pristine GCN is shown in Fig. 1. The structure of the unit cell contains three types of N atoms, such as N_{edge}, N_{inner}, and N_{bridge}, and two types of C atoms, such as C_{inner} and C_{bridge}, as shown in Fig. 1. The optimized value of the lattice constant was obtained to be 7.1 Å, which is comparable to experimental and theoretical findings reported in the literature [2,3,24,25].

In a 2×2 supercell, there are vacancies between 4 unit cells where different atoms and molecules can be embedded. To prevent interlayer interactions, a substantial vacuum distance of 18 Å was implemented along the Z direction. The relaxed structures of pristine GCN, Ni, Pd, and Pt-embedded GCN, and Ni, Pd, and Pt-embedded GCN with adsorbed NO gas are shown in Fig.2. From this Figure, it is observed that the Pd and Pt atoms are placed almost at the middle position (symmetrical place) of the GCN, whereas the Ni atom is almost asymmetrically placed in the GCN. This may be because the atomic radii of the Pd and Pt are greater than those of the Ni atom, which form a strong bond with the N atom of GCN. In addition, it is observed that the nitrogen atom of the NO gas is positioned above the vacancy site of the pristine GCN. At this site, the optimization energy is higher than at other possible positions of NO. Furthermore, the optimized structures show that the adsorption of NO gas on the GCN and TM-GCN system contributes to the structural distortion, and also noticeably changed shape of the systems from planar structure to buckled structure as the buckled structure is more stable than the planar structure [26]. The adsorption energy for the NO gas on pristine GCN and Ni, Pd, and Pt-embedded GCN were calculated using Eqs.1 and 2. The values thus obtained are presented in the third column of Table 1, and they are found to be 0.807, 4.270, 4.386, 4.560 eV for the NO gas on pristine GCN and Ni, Pd, and Pt embedded GCN respectively. In the last row of Table 1, nearly the same result has been reported by Gorai et al. [2] for Pt-embedded GCN. Based on this result, it can be inferred that the NO gas on GCN has low adsorption energy, whereas the

NO gas on Pt-embedded GCN has the highest adsorption energy. The adsorption energy is higher in the case of Pt-embedded GCN due to strong electronic hybridization between the Pt-5d orbitals and the N-2p states GCN. This acceptor-donor interaction leads to significant charge transfer from the metal's d-orbitals to the NO molecule, thereby enhancing the adsorption energy. In contrast, for Pd-embedded and Ni-embedded GCN, the d-orbitals are either fully occupied (Pd: $4d^{10}$) or more localized (Ni: $3d^8$), which limits their capacity for effective back-donation to the adsorbate. As a result, the weaker orbital overlap and reduced charge transfer lead to lower adsorption energies. The optimized nitric oxide bond length (d_{NO}) has been given in the first row (fifth column) of Table 1. It has been found that the bond length of this molecule changes when it is adsorbed by GCN and TM-GCN and this is in line with the previous work [2] as is seen in Table 1.

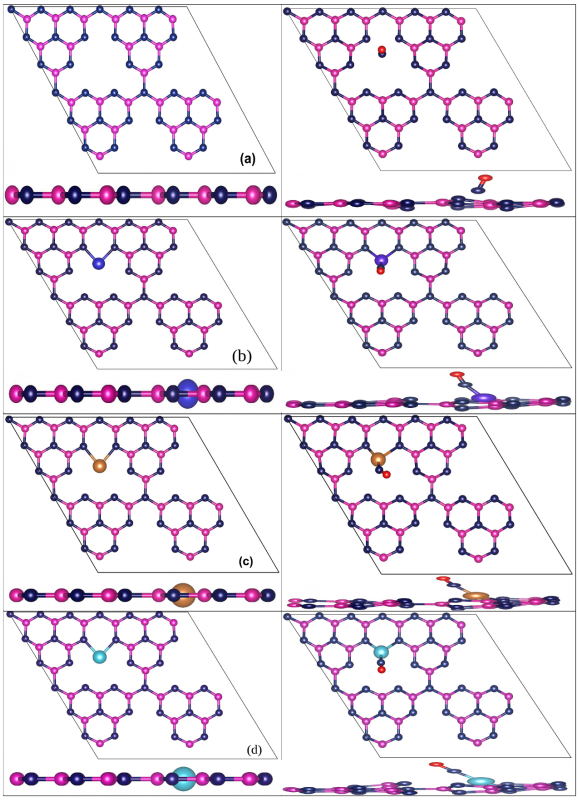

Figure 2: Optimized structure of pristine and TM-embedded GCN before and after NO adsorption (a) pristine GCN (b) Ni-embedded GCN (c) Pd-embedded GCN (d) Pt-embedded GCN.

The values for d_{NO} on GCN, Ni, Pd, and Pt-embedded value of d_{NO} on Pt-GCN suggests that the separation GCN were found to be 1.171, 1.173, 1.175, and 1.180 Å respectively (fifth column of Table 1). The maximum value of d_{NO} on Pt-GCN suggest that the separation of polarization of charge between N and O is greatest in Pt-embedded GCN [27]. Based on the above mentioned results, it can be concluded that NO interaction between the Pt-embedded GCN is stronger than the Ni and Pd-embedded GCN system. Further, the N atom of NO and the N_{edge} atom of GCN (before and after NO adsorption) both interact with the TM atom of TM-GCN. These bond distances have been shown in the last column of Table 1. On the other hand, the distance between N of GCN and TM also increases before and after the adsorption of NO. This indicates weak hybridization between N of GCN and TM. Additionally, the distance between Pt and N of GCN for NO adsorbed Pt-GCN is the largest compared to another case.

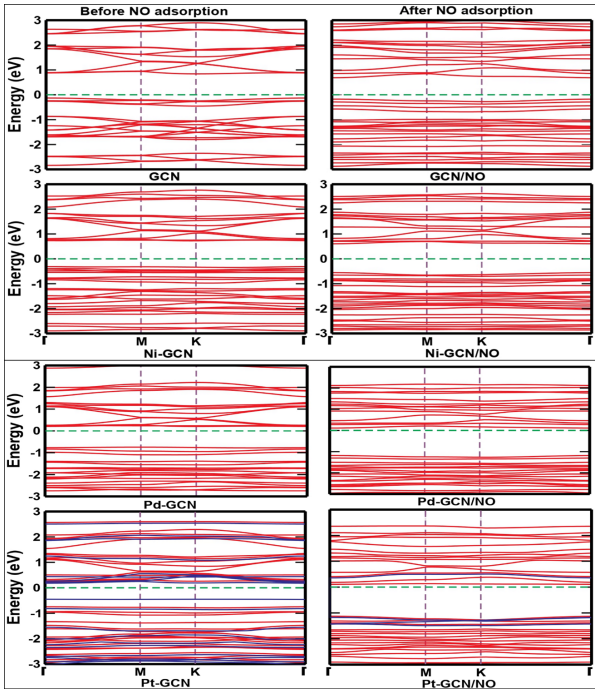

Figure 3: Spin-polarized electronic band structure of pristine GCN, Ni-embedded GCN, Pd-embedded GCN, and Pt-embedded GCN before and after NO adsorption.

To get the electronic properties of the pristine GCN, Ni, Pd, Pt-embedded GCN, NO adsorbed GCN, and NO adsorbed Ni, Pd, Pt-embedded GCN, we performed the electronic polarized band structure of above aforementioned system by GGA-PBE approximation. New energy states are noticed near the Fermi level when Ni, Pd, and Pt are embedded in GCN and after the adsorption of NO gas on the GCN monolayers. Asymmetry seen in spin-up and spin-down density of state calculations show that the magnetic characteristics

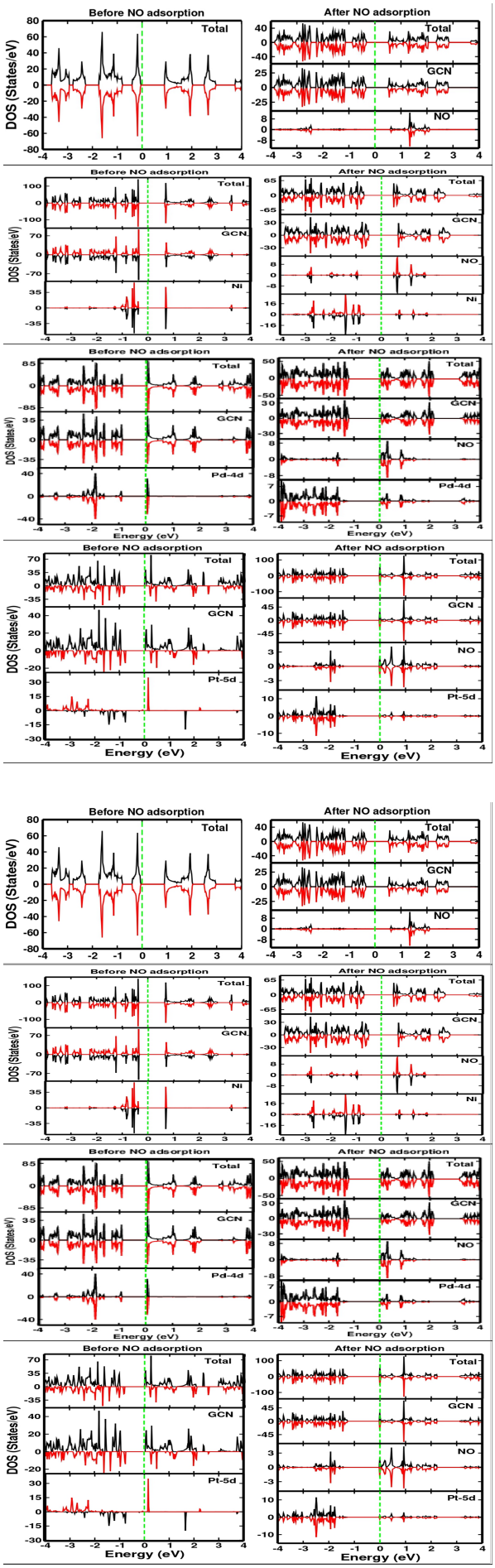

Figure 4

Figure 4: Spin-polarized total density of states and partial density of states for GCN, TM embedded GCN, NO adsorbed GCN, and NO absorbed TM-embedded GCN.

Figure 4 shows spin-polarized total density of states and partial density of states for GCN, TM-embedded GCN, NO adsorbed GCN, and NO-absorbed TM-embedded GCN. A similar type of result has been reported in previous study [2] also. The pristine GCN shows the semiconducting nature and it is observed that the band gap (E_g) for this system is 1.30 eV. It is lower than the experimental value (2.7 eV), since the PBE, the exchange-correlation functional method, usually underestimates the band gap energy. A similar sort of discrepancy has been found in the literature when the PBE functional was used for the band gap calculations [28–31]. The bandgap energy of the GCN significantly decreases after embedding Ni, Pd, and Pt in the GCN system, as shown in Table 1 and Fig.3.

The band lines corresponding to spin up and spin down of the pure and NO adsorbed pristine GCN, Ni, and Pd, Pt embedded GCN, are depicted in Fig. 3. The lines in both the conduction band (CB) and valance band (VB) of spin up and spin down of the pure and NO adsorbed pristine GCN, Ni, and Pd embedded GCN are seen overlapped showing symmetric, which indicates the materials to be non-magnetic. On the other hand, VB and CB band lines of the Pt-GCN and NO adsorbed Pt-GCN are asymmetric, indicating the materials to be magnetic with magnetic moments 1.4000, and 0.0001 μB respectively. Previous work [2] also shows similar values fairly confirming this result. It has been observed that after the NO adsorption on the Pt-embedded GCN, there is a considerable drop in the magnetic moment. This may be due to the strong hybridization between the 5d-orbitals of Pt with the p-orbital of the N atom of the NO.

To understand more about the electronic and magnetic properties resulting from NO adsorption on both pristine GCN monolayers and TM-GCN monolayers, spin-polarized partial density of states (PDOS) and total density of states (TDOS) have been calculated for all the systems. TDOS and PDOS before and after NO adsorption exhibit a significant change, as illustrated in Fig 4. There is significant increase in DOS in TM-embedded GCN with comparable to the GCN. In these systems, the embedded metals serve as a bridge, facilitating an enhanced hybridization between the gas molecule and the g-C_3N_4 monolayer.

The symmetric TDOS and PDOS were observed in pure and NO adsorbed pristine GCN, pure and

NO adsorbed Ni and Pd-embedded GCN (first, second, and third rows of Fig 4). There is symmetry observed between the spin-up and spin-down channels in pure and NO adsorbed pristine GCN, pure and NO adsorbed Ni, and Pd-embedded GCN in the first, second, and third rows of Fig 4. Thus, it can be inferred that these materials do not seem to exhibit magnetic behavior. In Pt-GCN, the absence of symmetry between the spin-up and spin-down states results in the manifestation of a magnetic moment in this system. However, NO adsorbed Pt-GCN shows almost symmetry between spin up and spin down in TDOS and PDOS diagrams, indicating almost negligible magnetic moment.

4 Conclusion

The adsorption behavior of the toxic gas NO on Ni, Pd, and Pt-embedded GCN has been studied using the first-principles method. It is evident from structural properties and adsorption analysis depicted in the optimized diagram that NO is physically adsorbed into GCN, whereas it is chemically adsorbed into Ni, Pd, and Pt-embedded GCN. Further, Ni is positioned asymmetrically, while Pd and Pt are symmetrically placed within the GCN cavity. Additionally, from adsorption energy calculations, we may say that NO tends to adsorb more on Pt-embedded GCN than on Ni, and Pd-embedded GCN. The band energy of all systems is found within the range of semiconducting materials. From the electronic properties that were calculated from the GGA-PBE DFT method, it can be inferred that GCN, TM-embedded GCN (TM=Ni, Pd), NO adsorbed GCN, NO adsorbed Ni and Pd embedded GCN are non-magnetic materials. Thus, like other pollutants as well as toxic gases, metal-embedded GCN has been seen to adsorb NO, as shown by other theoretical and experimental studies.

Acknowledgments

This work is supported by the International Science Program (NEP01), Uppsala University, Sweden for computing resources, and the partial financial aid for GNP is provided by the University Grants Commission (UGC Master Grants, Grant no. MRS-77/78-S&T-127), Nepal.

Author Contributions

Guna Nidhi Poudel: Conceptualization, Methodology, Investigation, Visualisation, Data curation, Formal analysis, Validation, Writing - original draft Pitamber Shrestha: Validation, Formal analysis. **Narayan Prasad Rijal:** Writing, review & editing. **Shriram Sharma:** Validation, Formal analysis. **Leela Pradhan Joshi:** Project administration, Formal analysis. **Rajendra Parajuli:** Resources, Software, Validation, Supervision, Formal analysis, Writing, review & editing.

Data Availability

The data that are used to create figures and tables are available upon request to the corresponding author.

Declarations and Conflict of Interest

There is no conflict of interest by the authors.

References

[1] L. Xu, Y. Liu, Y. Gui, Q. Zhang, and X. Chen. Adsorption property of co, no, and no2 gas molecules on co3-mose2 monolayer. *Sensors and Actuators A: Physical*, 319:112547, 2021.

[2] D. K. Gorai and T. K. Kundu. No adsorption on the os, ir, and pt embedded tri-s-triazine based graphitic carbon nitride: A dft study. *Applied Surface Science*, 590:153104, 2022.

[3] H. Basharnavaz, A. Habibi-Yangjeh, and S. H. Kamali. Fe, ru, and os–embedded graphitic carbon nitride as a promising candidate for no gas sensor: A first-principles investigation. *Materials Chemistry and Physics*, 231:264–271, 2019.

[4] M. Bowker. Automotive catalysis studied by surface science. *Chemical Society Reviews*, 37(10):2204–2211, 2008.

[5] M. J. Bojdys, J.-O. Müller, M. Antonietti, and A. Thomas. Ionothermal synthesis of crystalline, condensed, graphitic carbon nitride. *Chemistry– A European Journal*, 14(27):8177–8182, 2008.

[6] J. Neidhardt and L. Hultman. Beyond c3n4—fullerene-like carbon nitride: A promising coating material. *Journal of Vacuum Science Technology A*, 25(4):633–644, 2007.

[7] F. Su, M. Antonietti, and X. Wang. mpg-c3n4 as a solid base catalyst for knoevenagel condensations and transesterification reactions. *Catalysis Science Technology*, 2(5):1005–1009, 2012.

[8] J. Zhu, P. Xiao, H. Li, and S. A. Carabineiro. Graphitic carbon nitride: synthesis, properties, and applications in catalysis. *ACS Applied Materials Interfaces*, 6(19):16449–16465, 2014.

[9] J. Zhang, M. Grzelczak, Y. Hou, K. Maeda, K. Domen, X. Fu, M. Antonietti, and X. Wang. Photocatalytic oxidation of water by polymeric carbon nitride nanohybrids made of sustainable elements. *Chemical Science*, 3(2):443–446, 2012.

[10] G. Gao, Y. Jiao, F. Ma, Y. Jiao, E. Waclawik, and A. Du. Carbon nanodot decorated graphitic carbon nitride: new insights into the enhanced photocatalytic water splitting from ab initio studies. *Physical Chemistry Chemical Physics*, 17(46):31140–31144, 2015.

[11] Y. Wang, L. Liu, T. Ma, Y. Zhang, and H. Huang. 2d graphitic carbon nitride for energy conversion and storage. *Advanced Functional Materials*, 31(34):2102540, 2021.

[12] Y. Xu, S.-X. Jiang, W.-J. Yin, W. Sheng, L.-X. Wu, G.-Z. Nie, and Z. Ao. Adsorption behaviors of hcn, so2, h2s and no molecules on graphitic carbon nitride with mo atom decoration. *Applied Surface Science*, 501:144199, 2020.

[13] H. Basharnavaz, A. Habibi-Yangjeh, and S. H. Kamali. Adsorption performance of so2 gases over the transition metal/p–codoped graphitic carbon nitride: a dft investigation. *Materials Chemistry and Physics*, 243:122602, 2020.

[14] Z. Gu, Z. Cui, Z. Wang, K. S. Qin, Y. Asakura, T. Hasegawa, S. Tsukuda, K. Hongo, R. Maezono, and S. Yin. Carbon vacancies and hydroxyls in graphitic carbon nitride: Promoted photocatalytic no removal activity and mechanism. *Applied Catalysis B: Environmental*, 279:119376, 2020.

[15] H.-p. Zhang, A. Du, N. S. Gandhi, Y. Jiao, Y. Zhang, X. Lin, X. Lu, and Y. Tang. Metal-doped graphitic carbon nitride (g-c3n4) as selective no2 sensors: a first-principles study. *Applied Surface Science*, 455:1116–1122, 2018.

[16] H. Basharnavaz, A. Habibi-Yangjeh, and S. H. Kamali. A first-principle investigation of no2 adsorption behavior on co, rh, and ir-embedded graphitic carbon nitride: Looking for highly sensitive gas sensor. *Physics Letters A*, 384(2):126057, 2020.

[17] G. Kresse and J. Furthmüller. Efficient iterative schemes for ab initio total-energy calculations using a plane-wave basis set. *Physical Review B*, 54(16):11169, 1996.

[18] J. P. Perdew, M. Ernzerhof, and K. Burke. Rationale for mixing exact exchange with density functional approximations. *The Journal of chemical physics*, 105(22):9982–9985, 1996.

[19] H. J. Monkhorst and J. D. Pack. Special points for brillouin-zone integrations. *Physical review B*, 13(12):5188, 1976.

[20] G. Kresse and D. Joubert. From ultrasoft pseudopotentials to the projector augmented-wave method. *Physical Review B*, 59(3):1758, 1999.

[21] P. E. Blöchl. Projector augmented-wave method. *Physical Review B*, 50:17953–17979, 1994.

[22] E. Kroke, M. Schwarz, E. Horath-Bordon, P. Kroll, B. Noll, and A. D. Norman. Tri-striazine derivatives. part i. from trichloro-tri-striazine to graphitic c3n4 structures. *New Journal of Chemistry*, 26(5):508–512, 2002.

[23] S. Sun, S. Gu, J. Sun, F. Xia, and G. Chen. First principles investigation of the electronic properties of graphitic carbon nitride with different building block and sheet staggered arrangement. *Journal of Alloys and Compounds*, 735:131–139, 2018.

[24] H. Basharnavaz, A. Habibi-Yangjeh, and S. H. Kamali. A first-principles study on the interaction of co molecules with viii transition metalsembedded graphitic carbon nitride as an excellent candidate for co sensor. *Physics Letters A*, 383(21):2472–2480, 2019.

[25] J. Cui, S. Liang, X. Wang, and J. Zhang. First principle modeling of oxygen-doped monolayer graphitic carbon nitride. *Materials Chemistry and Physics*, 161:194–200, 2015.

[26] X. Ma, X. Li, M. Li, X. Ma, L. Yu, and Y. Dai. Effect of the structure distortion on the high photocatalytic performance of c60/g-c3n4 composite. *Applied Surface Science*, 414:124–130, 2017.

[27] K. Bai, Z. Cui, E. Li, Y. Ding, J. Zheng, C. Liu, and Y. Zheng. Adsorption of gas molecules on group iii atoms adsorbed g-c3n4: a firstprinciples study. *Vacuum*, 175:109293, 2020.

[28] Z. Wang, M. Chen, Y. Huang, X. Shi, Y. Zhang, T. Huang, J. Cao, W. Ho, and S. C. Lee. Self-assembly synthesis of boron-doped graphitic carbon nitride hollow tubes for enhanced photocatalytic nox removal under visible light. *Applied Catalysis B: Environmental*, 239:352–361, 2018.

[29] W. Xiong, S. Chen, M. Huang, Z. Wang, Z. Lu, and R.-Q. Zhang. Crystal-face tailored graphitic carbon nitride films for high-performance photoelectrochemical cells. *ChemSusChem*, 11(15):2497–2501, 2018.

[30] B. Zhu, L. Zhang, B. Cheng, and J. Yu. First principles calculation study of tri-s-triazine-based g-c3n4: a review. *Applied Catalysis B: Environmental*, 224:983–999, 2018.

[31] D. R. Lawati, H. K. Neupane, D. K. Chaudhary, P. Shrestha, R. P. Adhikari, L. P. Joshi, and R. Parajuli. Structural, mechanical, electronic and optical properties of mgzno3 perovskite: First-principles study. *Journal of Physics and Chemistry of Solids*, 181:111547, 2023.